Coarse recycled materials for the drainage and substrate layers of green roof system in dry condition: parametric study and thermal heat transfer

Mostafa Kazemi[1]*, Luc Courard[2], Julien Hubert[3]

Corresponding author*

1- Ph.D. Candidate, GeMMe Building Materials, Urban and Environmental Engineering (UEE), University of Liege, Liège, Belgium, E-mail: mostafa.kazemi@uliege.be

2- Full Professor, GeMMe Building Materials, Urban and Environmental Engineering (UEE), University of Liege, Liège, Belgium, Email: luc.courard@uliege.be

3- Postdoctoral researcher, GeMMe Building Materials, Urban and Environmental Engineering (UEE), University of Liege, Liège, Belgium, Email: julien.hubert@uliege.be

Abstract

The replacement of natural materials with recycled materials for green roof systems with drainage and substrate layers has scarcely been evaluated while it can be considered as a potential solution to reduce the overuse of natural resources. Moreover, optimizing green roof layers' thickness and evaluating the thermal resistance of drainage and substrate layers in dry state have rarely been taken into account. Therefore, the aim of this work was to assess the green roof layers' thermal resistance concerning ISO 9869-1 where the drainage and dry substrate layers are substituted with coarse recycled materials. A sensitivity analysis was conducted using WUFI software to optimize the thickness of different layers. As per the results, there was a narrow difference between the Rc-value of the proposed green roof made with coarse recycled materials and that of the control green roof without coarse recycled materials, (5.3%); so, recycled materials are recommended to be used for the rooftops due to their low bulk density and light weight. Moreover, the dry substrate layer's Rc-value was about twice that of the drainage layer of coarse aggregates due to deeper thickness of the former than the latter; however, considering the same thickness for the coarse aggregates and dry substrate layers, the Rc-value of the coarse aggregates was higher. Meanwhile, by simultaneously increasing the thickness of both layers, the model with an 18-cm substrate layer and a 6-cm drainage layer adequately provided the heat retention capacity required for the green roof system.

Keywords: Coarse recycled materials; substrate; drainage layer; thermal transfer modeling; parametric study.

1. Introduction

In recent decades, the rapid urbanization growth has been a challenge for the energy production sector to the point where the residential and commercial buildings in the European community account for 40% of primary energy consumption [1–8]. Given the increasing scarcity of fossil fuel and the environmental issues linked to their use, it has become an utmost necessity to appropriately design our buildings to improve their insulation henceforth reducing their energy consumption. The rooftop is of particular interest because it is one of the main sources of energy loss. Likewise, this has raised a demand for using appropriate materials with suitable design recommendations for roof applications to improve the insulation performance of rooftops. To achieve this goal, the green roof implementation instead of a conventional flat roof has been suggested to moderately improve the energy efficiency of dwelling houses in urban regions [1,9–15].

Of all types of green roof systems, the extensive green roof applies the smallest load to the rooftops due to its lower thickness and weight [16–18]. As environmentally-friendly building products, it is composed of the following layers: vegetation, substrate, filter, drainage and insulation [19,20]. The application of natural gravel aggregates as drainage layer of green roof was assessed by Wanielista and Hardin [21]. As per the experimental outputs, the atmospheric temperature increment contributed to an increase in the evapotranspiration process through the green roof system's depth once the natural gravel aggregate was employed for the drainage layer. The heat retention capacity of pebble and gravel aggregates as drainage layer was evaluated by Parizotto and Lamberts [22]. The results revealed that the heat retention capacity of green roof system was improved owing to the materials' diffusive properties used for the drainage and substrate layers. This resulted in retarding the heat transfer conduction and reducing the daily temperature fluctuation.

Natural coarse aggregates have proven to be able to provide an adequate water transmission ability for the drainage layer [23,24]. However, they have been overused in the construction industry and their intensive exploitation has had dire environmental consequences in the past decades [25–32]. This issue can be somewhat solved by the substitution of natural aggregates with recycled materials in the green roofs [33]. The water retention capacity of the green roofs can increase due to the higher porosity of recycled materials [34–36]. That same porosity is also responsible for the acceleration of the leakage of extra water from the green roof [37,38]. Pianella et al. [39] demonstrated that the green roof system's thermal resistance was dependant on the materials used for their layers. Besides, the lowest thermal conductivity was attained for the dry substrate, while it increased with increment of the substrate's moisture content. Recently, the thermal performance of green roof with a drainage layer made of perlite, expanded clay, and rubber crumbs was assessed by Cascone et al. [19]. According to the results, the diurnal temperature fluctuations of buildings with green roofs decreased compared to that of buildings with traditional roofs. This is due to the higher thermal inertia generated by the drainage and substrate layers. Another study by Coma et al. [1,40] demonstrated that, during the summer, a drainage layer made

of rubber crumbs provided more energy savings than one made with volcanic gravel. The application of pozzolana and rubber crumbs for the drainage layer of green roof was evaluated by researchers [1,40] during summer and winter periods. Better thermal performance was observed in the Mediterranean climate for the green roof system than conventional flat roof, particularly for the summer period, while the reverse was seen for the winter period. To solve this issue, they stated that an increase in the thickness of green roof layers might improve their thermal performance for the cold period. Following this, to assess the thermal performance of green roof layers, Kazemi et al. [11,41] performed a parametric study for green roof layers in which the rubber crumbs and pozzolana were simulated as drainage layer and their thermal performance was assessed during summer and winter periods. The WUFI software was used by Kazemi et al. [11,41] to simulate this configuration, which was suitable for analyzing the green roof layers' thermal resistance as already revealed by other researchers [42–44]. According to the modeling results, the fluctuation of temperature through the green roof's depth decreased with increment of the drainage and substrate layers' thickness. Besides, depending on the properties of green roof layers, a simultaneous thickness increase of drainage layer of pozzolana and substrate layer showed that the model with an 8-cm pozzolana layer and a 10-cm substrate layer was providing the best thermal performance for the rooftop for the winter and summer periods.

Based on the above, it is evident that although some researches have been carried out on the insulation performance of green roof systems, more extensive research is essential to optimize the green roof layers' thickness, particularly for layers produced with coarse recycled materials [1,11,40,41,45,46]. Moreover, European standards have never reported the optimum thickness for green roof layers [13,47]. Even though recycled coarse materials seem to be a suitable insulation material for green roof systems thanks to their great porosity [48–50], very little information is available on their thermal and insulating performances. So, in the present study, the thermal resistance of green roofs with a recycled coarse aggregates layer (drainage layer) and a substrate layer produced with coarse recycled materials was measured and evaluated in accordance with ISO 9869-1 [51]. Thereafter, the green roof layers' thermal properties were utilized for the simulation of green roof systems and the modeling data were validated with experimental data. After that, since the indicators for the thermal resistance assessment are related to the temperature value of materials [11,52–54], a sensitivity analysis on the influence of the drainage and substrate layers' thickness on the temperature distribution was performed. This parametric study allowed for the determination of the optimum thickness of both drainage and substrate layers to optimize the green roof systems' thermal performance.

2. Methodology

In this study, the initial heat conditions of drainage and dry substrate layers based on coarse recycled materials were obtained to analyze the green roof models' thermal performance. To assess the green roof layers' thermal performance in dry condition, the coarse aggregates and substrate were dried and kept in the oven at 40°C for 2 and 7 days, respectively, before starting the thermal

testing procedure. After drying the green roof materials, the dry substrate layer without recycled coarse aggregate and the natural coarse aggregates layer (drainage layer) were considered for the green roof specimen as a control specimen (Fig. 1). After that, both the substrate and drainage layers have been replaced by recycled materials. The dry and light mix of recycled bricks and tiles produced by Zincohum was used as substrate layer and the recycled coarse aggregates layer (drainage layer) were used as drainage layer (Fig 2).

(a) (b)

Fig. 1. Dry convectional materials for the control green roof: dry substrate without recycled bricks and tiles (a); natural coarse aggregates (b).

(a) (b)

Fig. 2. Dry recycled materials for the green roof: dry substrate produced with recycled bricks and tiles (a); recycled coarse aggregates (b).

The green roof's total thickness was 20 cm, with the drainage and substrate layers assumed to be 5 cm and 15 cm, respectively. The drainage layer is in charge of water transmission in the green roof system's bottom [55,56]. The EN 12620 [57] recommends that the coarse aggregates should not be smaller than 5 mm but on the other hand, they should not be too big given the shallow depth of the drainage layer (5cm). So, natural and recycled aggregates with a size of 7 mm were used for the drainage layer.

The proposed and the control green roof specimens were put in a 40 × 40 × 20 cm mini experimental mold as shown in Fig. 3(a). After that, the mold was placed in the thermal device's center between the hot and cold plates (Fig. 3(b)). The polyurethane foam was used to insulate the lateral panels of the experimental mold from the environment as shown in Figs. 3(a) and 4. Thereafter, the specimen's top and bottom were exposed to the applied temperatures using the hot and cold plates of the thermal device (Fig. 3(b)). This device was able to measure the green roof's thermal conductivity using a sensor installed at its bottom. A sketch of the different layers is

depicted in Fig. 4(a). The dry substrate and drainage layers were also tested separately to measure their thermal resistance. Natural and recycled materials were both considered. For example, the dry substrate layer composed of natural dry soil was put alone in the experimental mold and then in the thermal device to measure its thermal conductivity. This configuration is referred as SC15 (for 15 cm of dry substrate without coarse recycled materials). The same test has been done for the dry substrate composed of coarse recycled materials (SP15) as depicted in Fig. 4(b). After that, the 5-cm natural coarse aggregates layer (NCA5) was put alone in the experimental mold as depicted in Fig. 4(c). The same test has been done for the 5-cm drainage layer made of recycled coarse aggregates (RCA5).

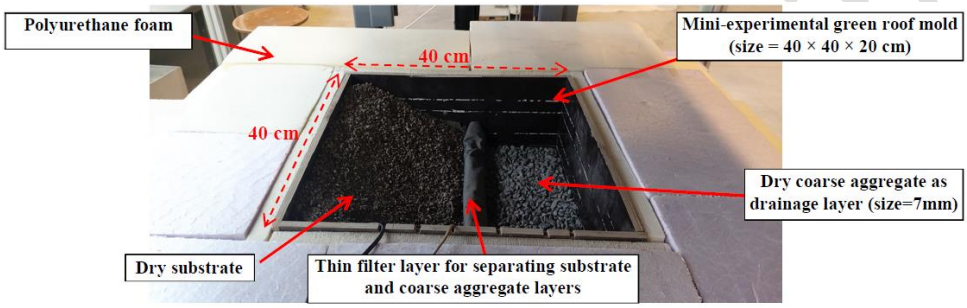

(a)

(b)

Fig. 3. Thermal device (a); drainage and substrate layers in the mini experimental green roof mold situated in the center of the thermal device (b).

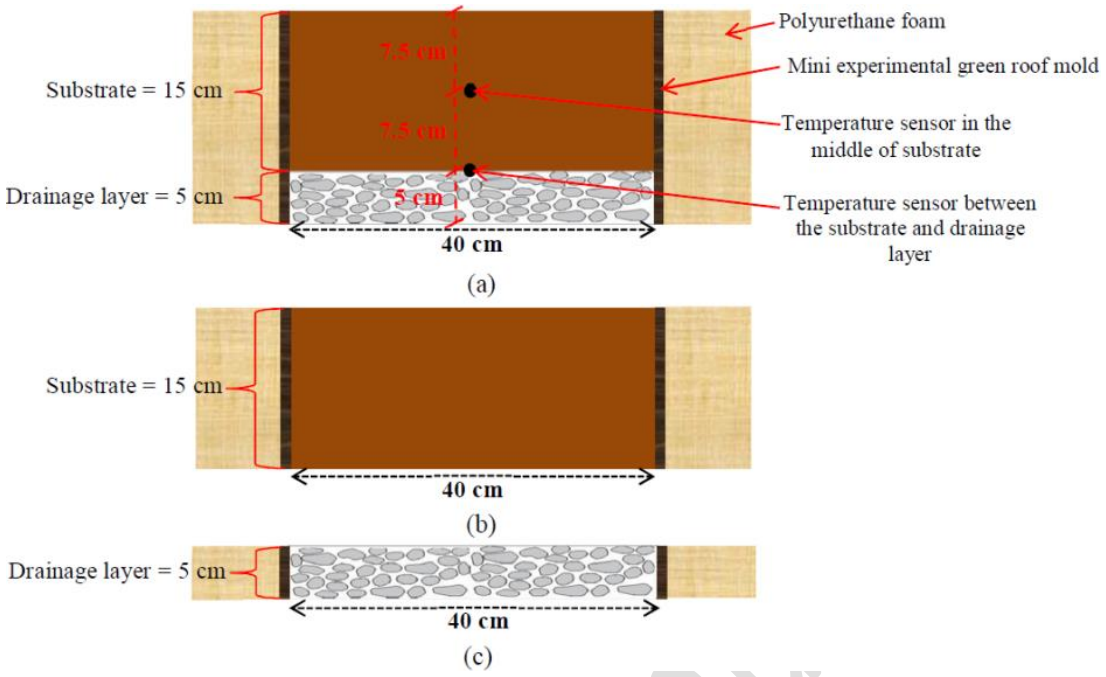

Fig. 4. Cross sectional schemes of 20-cm green roof layers: 5-cm natural coarse aggregates layer and 15-cm substrate layer (a); substrate layer (b); coarse aggregates layer (c).

The thermal conductivity measurement was carried out by means of the thermal device (Fig. 3(b)). The difference between the bottom and top temperatures of the green roof specimen (ΔT) was calculated using Eq. (1):

$$\Delta T = T_h - T_c \quad (1)$$

where T_h and T_c are referred to the temperatures in the hot and cold plates of thermal device, respectively (K).

Eq. (2) presents a formula to calculate the heat flow rate density, q, (W/m^2) according to Fourier's law:

$$q = \lambda.\frac{\Delta T}{l} \quad (2)$$

where l and λ are the green roof layers' thickness (m), and thermal conductivity (W/m·K), respectively.

In the thermal device, the heat flux sensor was installed in the center of the hot plate. Therefore, the location of this sensor was considered at the bottom of green roof (interior surface of green roof) as proposed by ISO 9869-1 [51].

As per the Average Method of ISO 9869-1 [51], the convergence of R_c-value (m^2K/W) was assessed using Eq. 3:

$$R_c = \frac{\sum_{t=0}^{m} \Delta T^t}{\sum_{t=0}^{m} q^t} \quad (3)$$

Where m and t are the minimum required measurement period (h) and time interval, respectively.

To stop the R_c-value measurement, the termination criteria in accordance with the Average Method of ISO 9869-1 [51] are presented below:

- Assuming the minimum test duration of 72 h is recommended.
- Less than ±5% difference should be obtained between the last two measurements of R_c-value.
- R_c-values during the first 67% of convergence period should not differ more than ±5 % from those during the last 67% of convergence period.

According to the Average Method of ISO 9869-1 [51], the difference between the interior and exterior surface temperature (temperature at the bottom and top of green roof) should be considered higher than 3 °C [58]. In addition to this, in order to use the Average Method, this surface temperature difference is recommended to be at least 5-10 °C [51,59,60]. So, the aforementioned difference was 7 °C in this study (the temperatures at the bottom and the top of green roof samples were 23.5 °C and 16.5 °C).

Two sensors were installed to measure the temperature at mid depth of the substrate and at the interface between the drainage and substrate layer (Fig. 4(a)). These temperature data were used to validate the modeling output (specifically the temperature distribution) at different depths in the green roof. Considering that the indicators for thermal resistance have been attributed to the temperature distribution through the materials' depth [11,52–54] , the temperature values were assessed by changing the drainage and substrate layers' depth to introduce the green roof layers' optimum thickness.

3. Properties and geometrical characteristics of green roof layers

The properties of drainage and substrate layers are presented in Table 1. The each layer's thermal conductivity was separately measured according to ISO 9869-1 [51] by means of the thermal device as explained in section 2 and depicted in Figs. 4 (b) and 4 (c). The ratio of the diffusion coefficients of water vapor in the building material and in the air is referred to the water vapor diffusion resistance Factor (μ). For coarse aggregates layers (porous materials), the μ-value could be close to 1 [61]. The diffusion coefficient of water vapor in the dry substrate was measured using the cup method which was adapted to EN 1015 [62]. Thereafter, the μ-values obtained for the SC15 and SP15 were 3.62 and 3.35, respectively.

Table 1. Properties of green roof layers.

Materials	Bulk density, ρ_s (kg/m^3)	Porosity	Specific heat capacity, Dry (J/kg K)	Thermal conductivity, Dry (W/m·K)	Water vapour diffusion resistance factor
SP15	855.7	0.482	880	0.15	3.62
SC15	944.1	0.4863	810	0.17	3.35
NCA5	1436.56	0.4167	770	0.114	1
RCA5	1164.47	0.4956	730	0.11	1

As presented in Table 1, the specific heat capacities obtained for the SP15 and SC15 were 810 and 880 J/kg K. The corresponding values for the drainage layer composed of natural and recycled coarse aggregates were 770 and 730 J/kg K. These were close to the values for dry soil and dried aggregates [63,64].

The specific heat capacity of the coarse aggregates and substrate was obtained using the Calorimetric method which was compatible with ASTM D4611-16 [65]. This parameter is the amount of the heat needed to increase the temperature of 1 kg of mass by 1 °C [66]. It is used to calculate the energy change associated with a temperature change. In most cases, the specific heat capacity of the substrate has been determined by the simplest and oldest approach namely the calorimetric method [67]. In this method, a substance can be heated to a particular temperature, and then it should quickly be mixed into a liquid medium of known temperature and known specific heat [68]. As per the law of conservation of energy, the heat lost by the substance should be equal to the heat gained by the liquid. By knowing the masses involved, the changes in temperatures, and the specific heat of the liquid, the unknown specific heat may be easily calculated.

Figs. 5 (a) and 5(b) are the schematic representations of the typical calorimeter method. To attain the dry substrate's specific heat capacity, its mass (W_s) was weighed. Then, the mass of water inside of the beaker (W_w) was measured. Later on, the substrate was put inside of the closed tube which was hung in water to prevent it from touching the sides and bottom of the beaker (Fig. 5 (a)). Thereafter, the beaker was exposed to high temperature using the boiler until the water reached boiling point. When the temperature of boiling water remained constant, the tube was kept in the beaker for 10 min to make the temperature of substrate equal to that of boiling water. This temperature was recorded using the thermometer as the initial temperature of dry substrate (T_s). The temperature of the same amount of water in ambient temperature was also measured using another thermometer (T_w) as shown in Fig. 5 (b). After ensuring that the substrate was heated evenly, the closed tube including dry substrate was brought out of the beaker in Fig. 5(a) and it was put inside of water with ambient temperature as shown in Fig. 5 (b). Later on, a stirrer was used to equalize the temperature of the water and the closed tube containing the dry substrate. In these conditions, the temperature of water in the beaker (Fig. 5 (b)) increased and its highest amount was recorded as the equilibrium temperature of mixed water and dry substrate (T_e). The same process was carried out once again to attain the specific heat capacity of the coarse aggregates for the drainage layer. Fig. 5 (c) shows the instruments used for measuring the specific heat capacity of substrate and coarse aggregates.

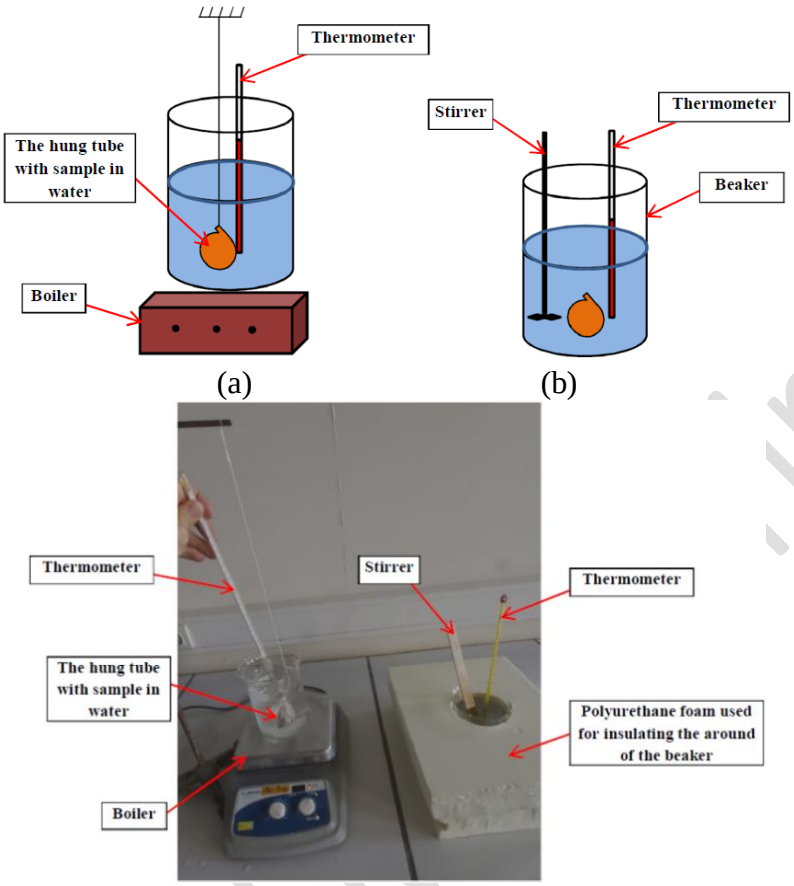

Fig. 5. Schematic representation for the calorimeter method: tube with sample in boiling water (a); tube in water at ambient temperature (b); instruments used for attaining the specific heat capacity of materials (c).

To measure the specific heat capacity of coarse aggregates and substrate, their heat transferred was determined by means of Eq. 4:

$$Q = c.m.\Delta T \quad (4)$$

where Q is change in heat (J), m is mass (g), c is specific heat capacity (J/g°C), and ΔT is the change in temperature (°C).

According to the principle of conservation of energy, for instance, the heat transferred of substrate (Q_s) could be considered equal to that of water (Q_w) as presented in Eq. 5:

$$Q_w = Q_s \quad (5)$$

Eq. 6 was obtained from Eqs. 4 and 5:

$$c_w.m_w.\Delta T_w = c_s.m_s.\Delta T_s \quad (6)$$

where c_w and c_s were the specific heat capacity of water and substrate, respectively.

By rearranging Eq. 6, Eqs. 7 and 8 were obtained to calculate the specific heat of the substrate:

$$c_s = \frac{c_w.m_w.\Delta T_w}{m_s.\Delta T_s} \quad (7)$$

$$c_s = \frac{c_w.m_w.(T_w - T_e)}{m_s.(T_e - T_s)} \quad (8)$$

The details and geometrical characteristics of the different green roof configurations are presented in Table 2. As already stated, the proposed and control green roof specimens (SP15-RCA5 and SC15-NCA5) were tested by means of the thermal device. After measuring the green roof specimens' thermal resistance for 7 days, two dimensional (2D) simulation were performed using the version 4.2 of WUFI software as seen in Fig. 6 and their results were compared with the experimental outputs. The properties of the dry substrate and drainage layers in Table 1 were introduced in the software and the boundary conditions imposed were the same exact temperatures applied to the green roof specimens using the hot and cold plates. The fine gird available in WUFI software was automatically considered through the depth of green roof to effectively validate the numerical models with experimental outputs. After validation, the drainage and substrate layers' depth influence over the temperature distribution in the green roof was analyzed. Regarding this, while keeping constant the thickness of substrate, the thickness of the drainage layer was changed to 4, 6, 7, and 8 cm for both proposed and control green roof models. In the next step, while keeping constant the thickness of the drainage layer, the thickness of substrate was changed to 12, 18, and 21 cm. Finally, while keeping constant the thickness ratio of substrate to drainage layer (3), the thicknesses of drainage and substrate layers were both changed simultaneously as presented in Table 2.

Table 2. Details and geometrical characteristics of green roofs.

No.	Specimen	Thickness (cm)	
		Substrate	Drainage layer
1	SC[a]15-NCA[b]4	15	4
2	SC15-NCA5	15	5
3	SC15-NCA6	15	6
4	SC15-NCA7	15	7
5	SC15-NCA8	15	8
6	SC12-NCA5	12	5
7	SC18-NCA5	18	5
8	SC21-NCA5	21	5
9	SC12-NCA4	12	4
10	SC18-NCA6	18	6
11	SC21-NCA7	21	7
12	SP[c]15-RCA[d]4	15	4
13	SP15-RCA5	15	5
14	SP15-RCA6	15	6
15	SP15-RCA7	15	7
16	SP15-RCA8	15	8
17	SP12-RCA5	12	5
18	SP18-RCA5	18	5
19	SP21-RCA5	21	5
20	SP12-RCA4	12	4
21	SP18-RCA6	18	6
22	SP21-RCA7	21	7

[a] Substrate without coarse recycled materials
[b] Natural coarse aggregate
[c] Substrate with coarse recycled materials
[d] Recycled coarse aggregate

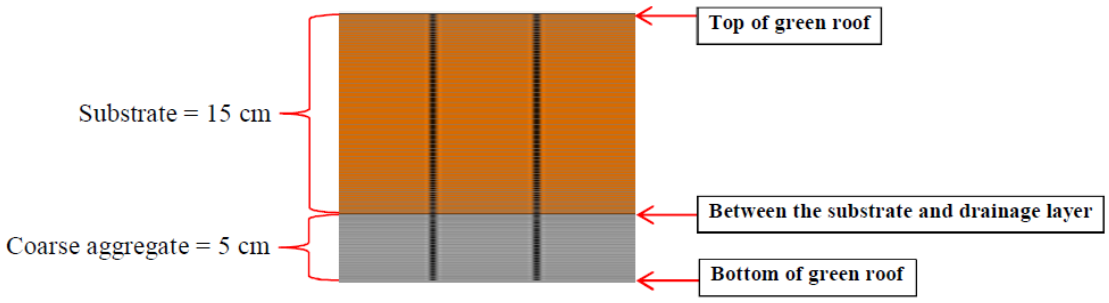

Fig. 6. 2D green roof model built by means of WUFI software.

4. Results and discussion

4.1. Heat flow measurement based on ISO 9869-1 [51]

The green roof layers' thermal conductivity was attained by means of the thermal device as seen in Fig. 7. After that, the R_c-values of all specimens in Fig. 4 were calculated using Eq. 3. The results of R_c-values given in Fig. 8 were assessed in accordance with the criteria of Average Method of ISO 9869-1 [51].

As per the first criterion given by ISO 9869-1 [51], the minimum test duration of 72 h (3 days) should be considered for the thermal performance monitoring of specimens to achieve the convergence of R_c-value. The test durations of all specimens are presented in Table 3. For the RCA5 and NCA5, the last 76 h of their test duration was assumed to assess the convergence of R_c-value. For the SP15 and SC15, the last 75 h and last 116 h of their test duration were assessed, respectively. The last 120 h of test duration of the proposed and control green roof specimens (SP15-RCA5 and SC15-NCA5) was assumed to evaluate the R_c-value convergence.

The R_c-values obtained 24 h before the termination of heat flow measurement for SP15-RCA5, SC15-NCA5, SP15, SC15, RCA5, and NCA5 were 1.27, 1.42, 0.94, 1.38, 0.44, and 0.443 m^2K/W, respectively. These values, for the same specimens, at the end of the heat flow measurement were 1.3, 1.4, 0.93, 1.4, 0.446, and 0.443 m^2K/W. A comparison between the results showed that the difference between data 24 h before the termination of heat flow measurement and at the end of the heat flow measurement was 2.4% at most, which is less than the 5% recommended by ISO 9869-1 [51].

In the convergence duration, presented in Table 3, the first 67% of R_c-value for SP15-RCA5, SC15-NCA5, SP15, SC15, RCA5, and NCA5 was averagely attained at 1.27, 1.4, 0.93, 1.036, 0.449, and 0.441 m^2K/W, respectively. The last 67% of R_c-value for the same specimens was on average about 1.32, 1.4, 0.94, 1.043, 0.446, and 0.44 m^2K/W. Therefore, the difference between the first and last 67% of R_c-value was of 3.9% at most, which is less than 5% as recommended by ISO 9869-1 [51]. As a consequence, R_c-values of all specimens were satisfactorily converged after meeting the termination criteria of the Average Method given by ISO 9869-1 [51].

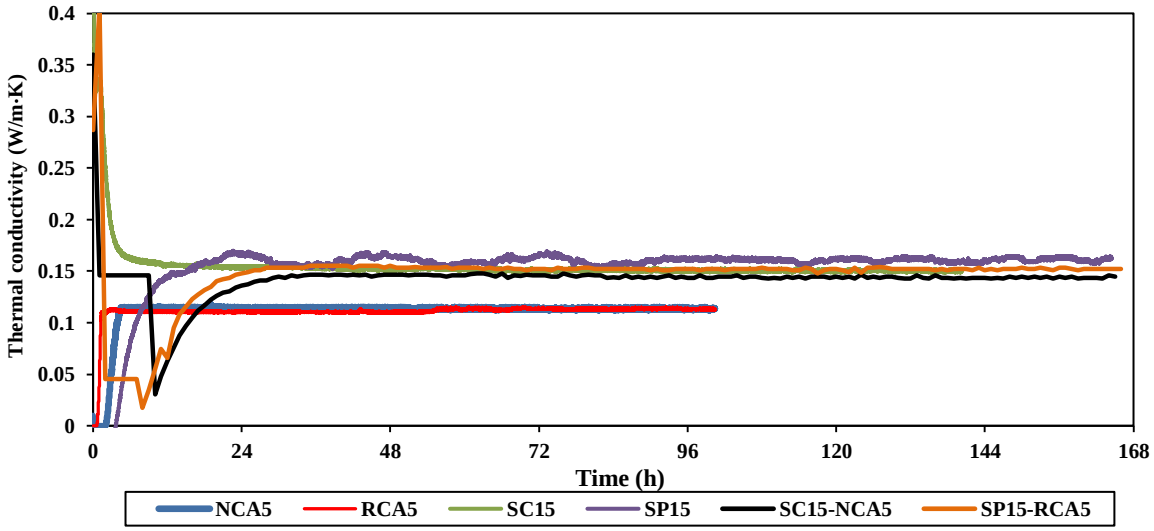

Fig. 7. Thermal conductivity of green roof layers.

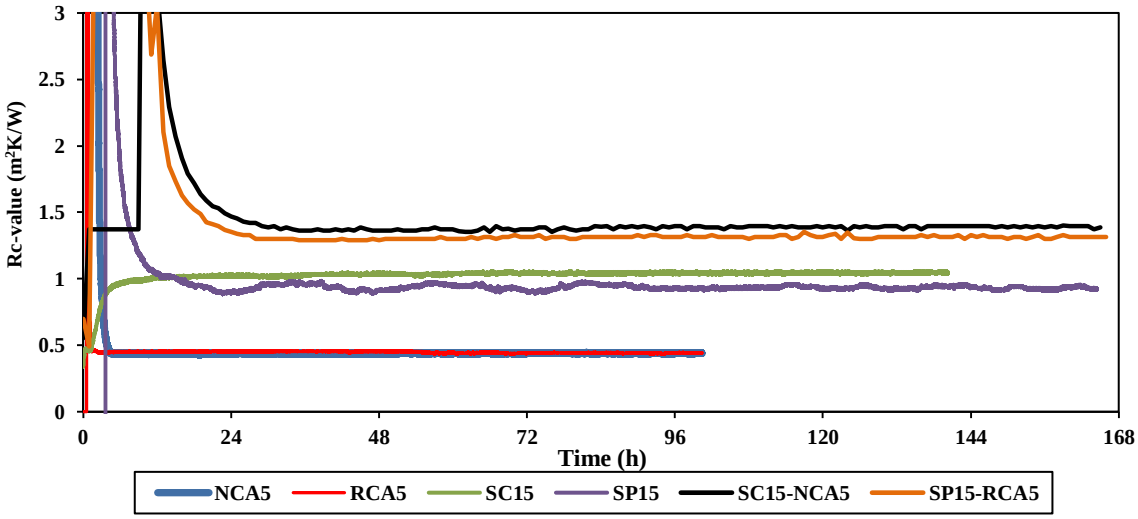

Fig. 8. Rc-value of green roof layers.

Table 3. Thermal properties of green roof layers.

Specimens	Test duration (h)	Convergence duration (h)	Thermal conductivity (W/m·K)	Rc-value (m^2K/W)
NCA5	101	76	0.114	0.44
RCA5	101	76	0.11	0.446
SC15	140	116	0.15	1
SP15	165	75	0.16	0.94
SC15-NCA5	165	120	0.142	1.38
SP15-RCA5	166	120	0.151	1.31

4.2. Thermal performances of green roof layers

The green roof layers' thermal conductivity and Rc-value are presented in Table 1. The thermal transmission and resistance of materials can be assessed using the thermal conductivity and Rc-value, respectively [39,69]. As presented in Table 1, the thermal conductivity of recycled and natural coarse aggregates layers (RCA5 and NCA5) was near to 0.11 W/m·K. Their Rc-values were also near to 0.44 m^2K/W and there was no difference between their thermal insulation performance, while the properties of natural and recycled coarse aggregates were different to each other. Concerning this, it is noteworthy that air within the voids can improve the heat resistance of building materials [11,41,70–72] and the thermal insulation of drainage layer was highly affected by the air-voids among coarse aggregates. Therefore, due to the heat resistance effect of air-voids, dominating that of coarse aggregate types, there was no difference between Rc-values of NCA5 and RCA5.

The results demonstrated that the thermal conductivity of the SP15 (0.16 W/m·K) was slightly higher than that of the SC15 (0.15 W/m·K), while the Rc-value of SP15 was slightly lower than the one of SC15 (6.4 %). This difference showed a slightly better thermal resistance for SC15 than for SP15. It can be inferred that the heat resistance ability of porous coarse recycled materials was a bit lower than that of dry soil particles and there is more air trapped within the former than within the latter, even though it only led to a narrow difference between the Rc-values of SC15 and SP15.

A comparison between the proposed and the control green roofs (SP15-RCA5 and SC15-NCA5) showed that the Rc-value of the former was slightly lower than that of the latter (5.3%). This narrow difference could be attributed to the thermal insulation resistance of the SC15 and SP15 as already described.

It is worth underlying that although the Rc-value of dry substrates (SC15 and SP15) was about twice greater than the one of the coarse aggregate layers (NCA5 and RCA5), it should be kept in mind that the former was three times as thick (15 cm) as the latter (5 cm). It means that, due to high heat resistance of air-voids among aggregates [1,11,41], the coarse aggregates layer has better thermal insulation performance than the dry substrate layer once they have equal thickness.

4.3. Comparison between the experimental and modeling results

The temperature fluctuations at different depths of the green roof models implemented in the WUFI software were compared with those of the SP15-RCA5 and SC15-NCA5 specimens. As seen in Figs. 9 and 10, the solid lines and dashed lines represent the temperature distribution in the green roof specimens and models, respectively. Since the location between the drainage and substrate layer was near to the hot plate of the thermal device and on the other hand, the middle of substrate was near to the cold plate, the temperature between the drainage and substrate layer was obtained higher than that in the middle of substrate as expected.

During the convergence duration (last 5 days of the test duration), the average value of temperatures reached in the middle of the substrate layer was 20.16 °C and 19.7 °C for the control specimen and 2D model (SC15-NCA5), respectively (Fig. 9). The corresponding values at the

interface between the substrate and the natural coarse aggregates layer were 22.15 °C and 21.64 °C. On the other hand, during the convergence duration, the average value of temperature in the middle of the substrate layer was 19.9 °C and 19.4 °C for the proposed specimen and 2D model (SP15-RCA5), respectively (Fig. 10). The corresponding values at the interface between the substrate and recycled coarse aggregate layer were 21.76 °C and 21.27 °C. Therefore, the difference between the temperature through the depth of the specimens and 2D models was lower than 2.6%. Moreover, the general trends of temperature distribution in the 2D models were nearly identical to those of the experimental specimens. In brief, the 2D green roof models' thermal performance was reliably validated via comparisons of the modeling outputs and experimental results.

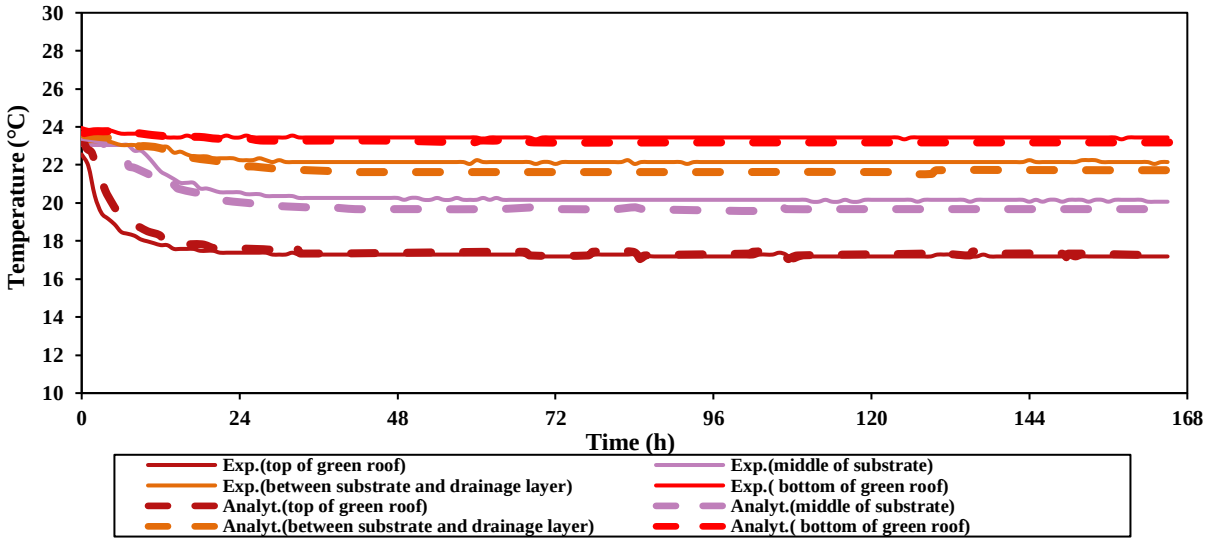

Fig. 9. Experimental results of the SC15-NCA5 specimen and its modeling outputs.

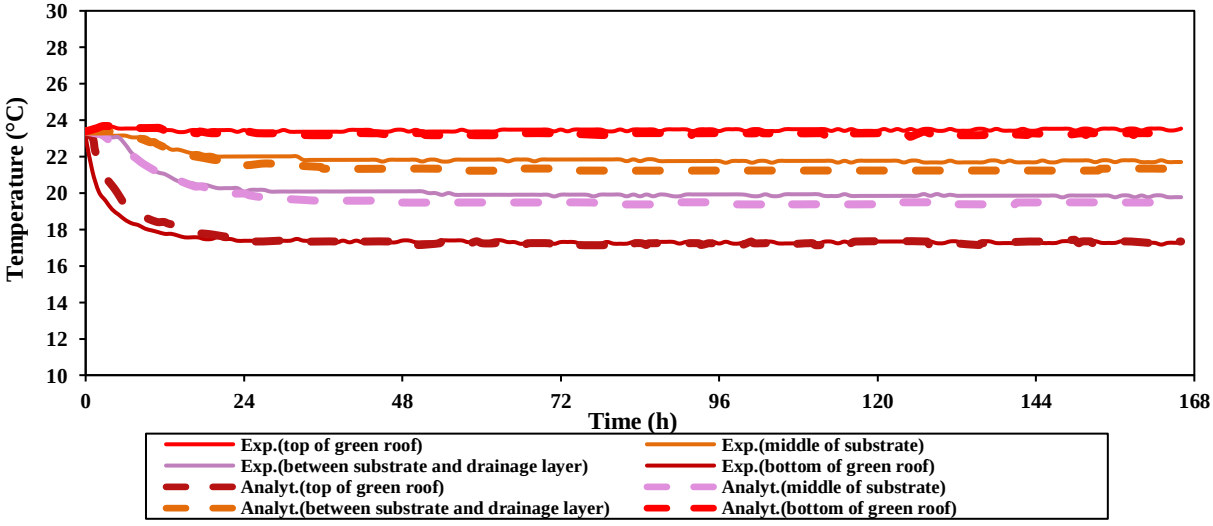

Fig. 10. Experimental results of the SP15-RCA5 specimen and its modeling outputs.

4.4. Parametric study

4.4.1. Thickness of drainage layer

The green roof's thermal resistance can be influenced by changing the thickness of its layers [11,41,73]. Considering this, to analyze the influence of coarse aggregates over the green roofs' thermal performance, the dry substrate layer's depth was assumed constant (15 cm) and the coarse aggregates layer's depth was changed from 5 cm to 4 cm, 6 cm, 7 cm, and 8 cm (Figs. 11 and 12), and then the optimum thickness of the coarse aggregates layer as a drainage layer was determined for both the SP15-RCA5 and SC15-NCA5 models once the general trends of temperature in their depth became stable.

The average temperature values through the depth of the models during the convergence duration are presented in Fig. 13. Since the bottom of green roof models was exposed to higher temperature (temperature of the hot plate in the thermal device), increasing the coarse aggregates layer's thickness decreased the average temperature at the interface between the drainage and the substrate layer similarly to what revealed in the middle of substrate layer. However, there was no significant change in the temperature distributions in some cases. For instance, the average value of the temperature at the interface between the drainage and substrate layer for the control models with 8-, 7-, and 6-cm natural coarse aggregates layer was about 21.2 °C. In addition, the temperature in the middle of the substrate layer for the control models with 8-, 7-, and 6-cm natural coarse aggregates layer was about 19.3 °C. Therefore, in the case of natural coarse aggregates, the increment of the drainage layer's depth above 6 cm yields no change in the temperature distribution.

The average value of the temperature at the interface between the drainage and substrate layer for the proposed models with 8-, 7-, and 6-cm recycled coarse aggregate was 20.8 °C. The temperature in the middle of the substrate for the models with 8-, 7-, and 6-cm dry substrate was about 19.2 °C. The same conclusions can thus be reached for the recycled coarse aggregates than for the natural coarse aggregates. In brief, by assuming the substrate layer with a constant depth, the 6-cm drainage layers of natural or recycled coarse aggregates could be considered the best configuration for the drainage layer. Moreover, as shown in Fig. 8, there was a negligible difference between the recycled and natural coarse aggregates' thermal resistance owing to the participation of air-voids among them to generate the insulation layer similar to what other researchers concluded [41,70–72]. On the other hand, the weight of 6-cm drainage layer of natural coarse aggregates is equal to 86.19 kg/m^2 according to the bulk density of materials presented in Table 1. The corresponding value for the 6-cm drainage layer of recycled coarse aggregates is 69.88 kg/m^2. Therefore, the recycled coarse aggregates are recommended for the drainage layer due to their lower bulk density and lighter weight, contributing to apply lower load to the top of structures as suggested by Teemusk and Mander [18].

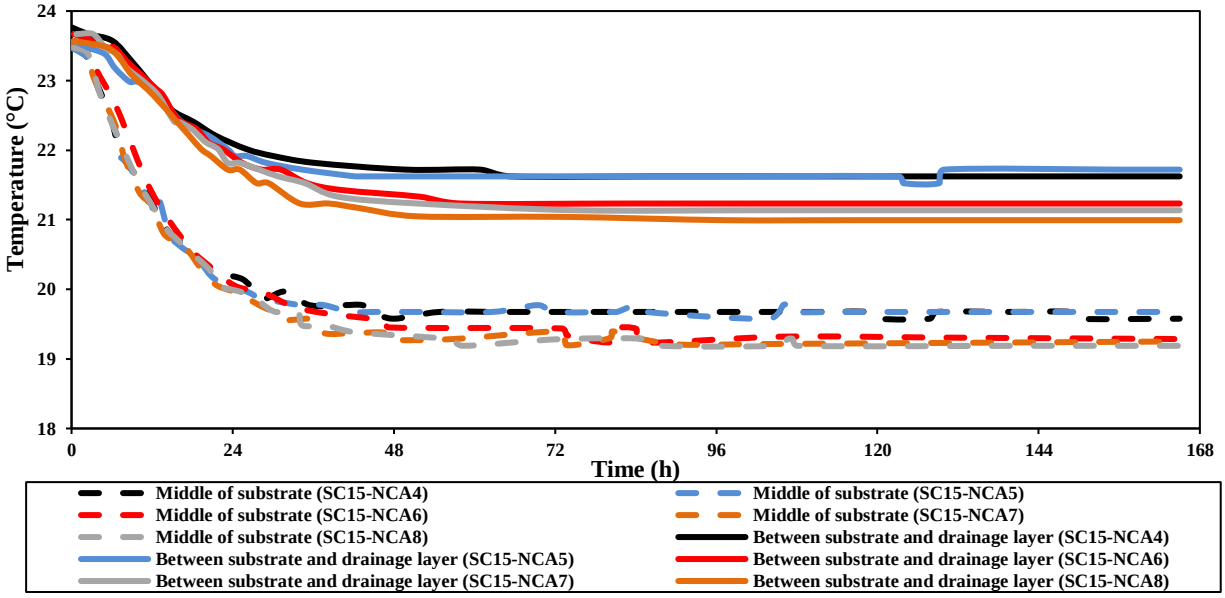

Fig. 11. Temperature distribution in the control models (change in the drainage layer's depth).

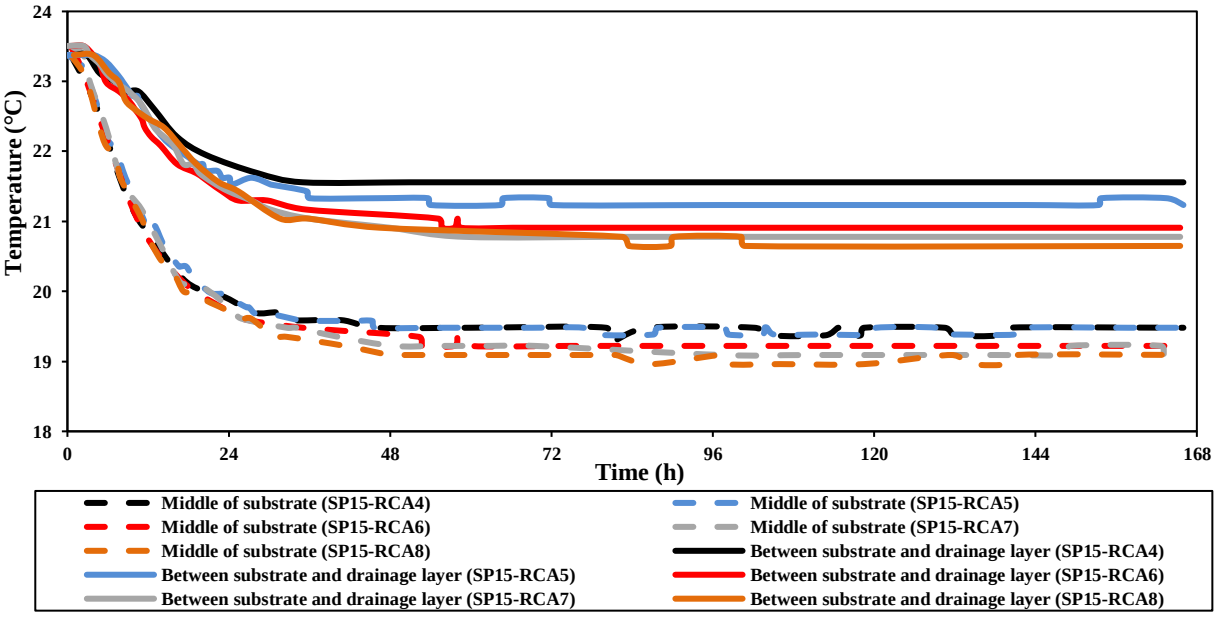

Fig. 12. Temperature distribution in the proposed models (change in the drainage layer's depth).

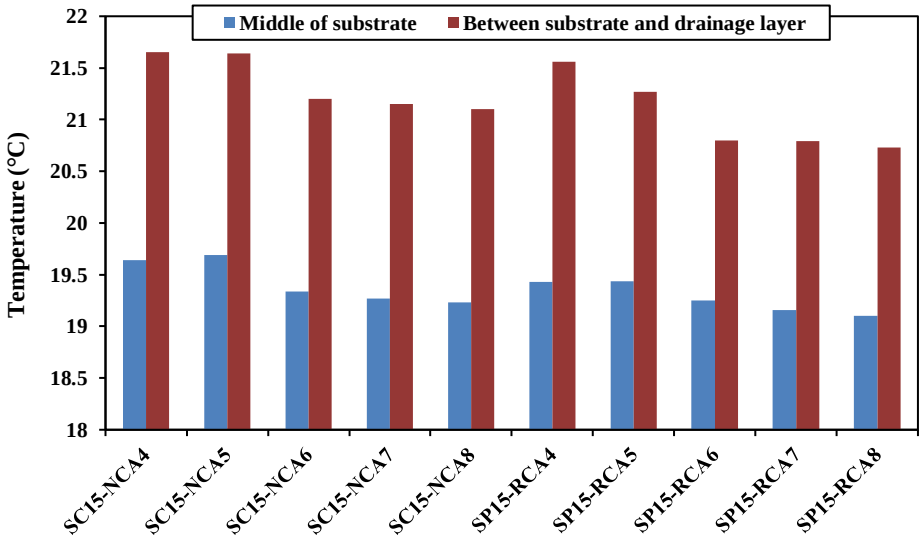

Fig. 13. Temperature in the depth of green roof models (change in the drainage layer's depth).

4.4.2. Thickness of substrate

To evaluate the influence of the dry substrate (substrate layer) over the green roof models thermal performance, the drainage layer's depth was assumed constant (5 cm) and the substrate's depth was changed from 15 cm to 12 cm, 18 cm, and 21 cm. After analyzing the modeling outputs given in Figs. 14 and 15, the dry substrate layer' optimum thickness was determined. The temperature average values through the green roof models' depth during the convergence duration are depicted in Fig. 16.

According to the results, the average value of temperature through the green roof layers' depth increased with increment of the dry substrate layer's thickness. However, no significant change was observed in the temperature distribution in the green roof's depth for deeper substrate owing to its high diffusion properties [22]. For example, the average value of the temperature in the middle of the substrate for the control models with 18- and 21-cm dry substrate layer was about 19.9 °C. Moreover, the temperature at the interface between the drainage and substrate layer for the control models with 18- and 21-cm dry substrate layer was close to 21.8°C, demonstrating the fact that the temperature distribution in green roof layers remained constant for the substrate with a thickness of more than 18 cm.

The temperature in the middle of the substrate for the proposed models with 21- and 18-cm dry substrate was about 19.7 °C. The temperature at the interface between the recycled coarse aggregates layer and substrate layer for the proposed models with 21- and 18-cm dry substrate was 21.6 °C. Therefore, the temperature distribution for the proposed models with 21- and 18-cm dry substrate was found to be the same once the thickness of recycled coarse aggregate layer was kept constant (5 cm).

In general, the radiation of heat in green roof layers was affected with the increment of the dry substrate's depth similarly to what Eksi et al. [74] concluded and SC18-NCA6 and SP18-RCA6 models were found to be the optimum design. However, by ignoring the slight difference between the Rc-value of SC15 and SP15, the proposed green roof (SP18-RCA6) can be regarded as the optimum design of systems for the rooftop due to its adequate heat resistance.

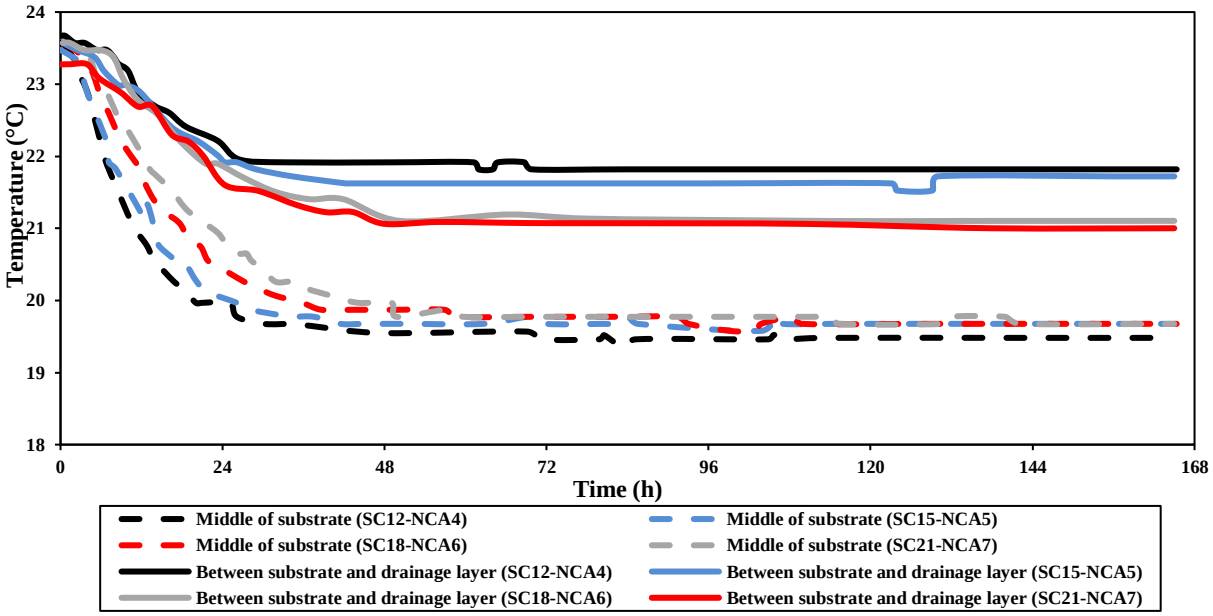

Fig. 14. Temperature distribution in the control models (change in the substrate layer's depth).

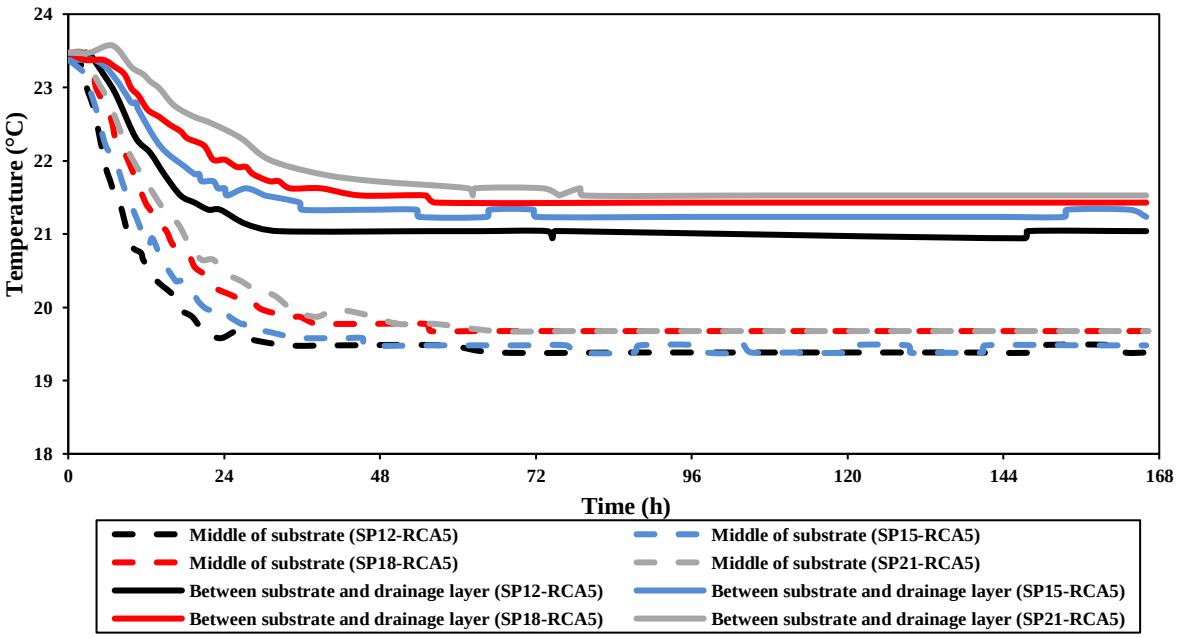

Fig. 15. Temperature distribution in the proposed models (change in the substrate layer's depth).

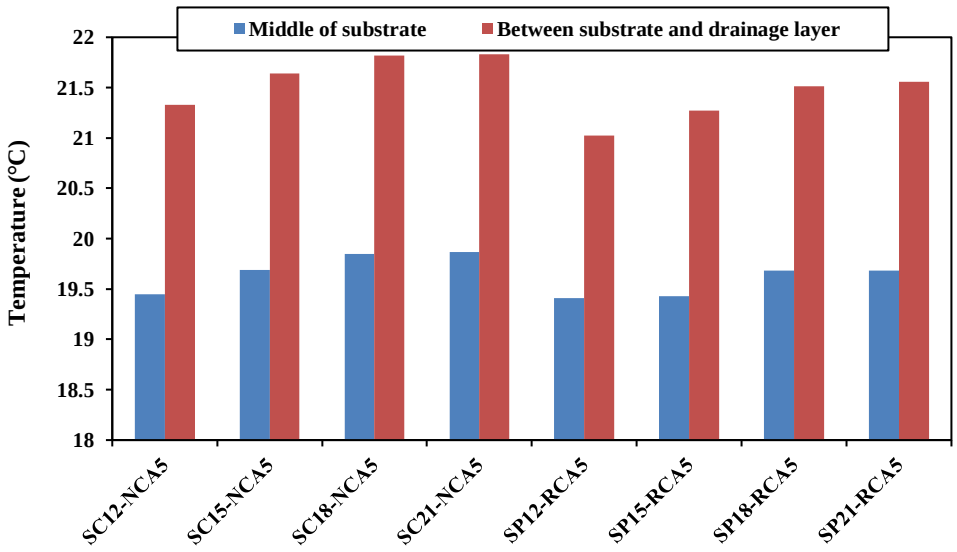

Fig. 16. Temperature in depth of green roof models (change in the substrate layer's depth).

4.4.3. Constant thickness ratio of dry substrate to drainage layer (3:1)

As shown in Figs. 17 and 18, for the proposed and the control models (SP15-RCA5 and SC15-NCA5), the thickness of the coarse aggregates and the dry substrate layers were simultaneously modified, while keeping constant the thickness ratio of substrate to drainage layer (3). Regarding this, the 5-cm coarse aggregates layer and 15-cm dry substrate layer were changed to 4-cm coarse aggregate layer and 12-cm dry substrate (SC12-NCA4 and SP12-RCA4), 6-cm coarse aggregate layer and 18-cm dry substrate (SC18-NCA6 and SP18-RCA6), and 7-cm coarse aggregate layer and 21-cm dry substrate (SC21-NCA7 and SP21-RCA7).

As per the modeling outputs, the temperature at the interface between the dry substrate and recycled coarse aggregate layer slightly increased, while the temperature decreased in the middle of the dry substrate by simultaneously increasing the thickness of both layers, owing to the thermal protection generated by deeper layers as demonstrated by Eksi et al. [74]. However, in some cases, no change was found in the temperature distribution in the green roof's depth for deeper layers (Figs. 17 and 18). Concerning this, the average values of temperature in the middle of the dry substrate layer and at the interface between the dry substrate and coarse aggregates layer during the convergence duration were presented in Fig. 19. In the middle of the dry substrate layer, a temperature of 19.5 °C was obtained for the control model with 4-cm natural coarse aggregates layer and 12-cm dry substrate (SC12-NCA4). The corresponding temperature for the control model with a 5-cm natural coarse aggregates layer and a 15-cm dry substrate layer (SC15-NCA5) was 19.7 °C. By increasing the thickness of the natural coarse aggregates layer and the dry substrate layer, the temperature remained constant (19.7 °C) for the SC18-NCA6 and SC21-NCA7 models. At the interface between the substrate and drainage layer, a temperature of 21.9 °C was attained for the control model with a 4-cm natural coarse aggregates layer and a 12-cm dry substrate layer

(SC12-NCA4). The corresponding temperature was of 21.7 °C for SC15-NCA5. For the control models with deeper thicknesses (SC18-NCA6 and SC21-NCA7), the temperature obtained was 21.1 °C. Therefore, there was no significant difference between the results of SC18-NCA6 and SC21-NCA7 models.

For the proposed models of SP12-RCA4 and SP15-RCA5, the average value of temperature at the interface between the dry substrate and recycled coarse aggregates layer was about 21.3 °C. By increasing the layers' thickness, the corresponding temperature was 21 °C for the SP18-RCA6 and SP21-RCA7 models. The temperature in the middle of the dry substrate layer for the SP12-RCA4 and SP15-RCA5 models was 19.2 °C and 19.4 °C. This temperature remained constant (19 °C) for the SP18-RCA6 and SP21-RCA7 models. Therefore, no significant change was observed between the results of the SP18-RCA6 and SP21-RCA7 models, similar to what was obtained for the control models between the SC18-NCA6 and SC21-NCA7 models. On the other hand, the weight of the control green roof with optimized layers (SC18-NCA6) is equal to 240 kg/m^2 according to the bulk density of materials presented in Table 1. Nearly the same value was obtained for the proposed green roof with optimized layers (SP18-RCA6). As a result, the proposed and the control models with a 6-cm coarse aggregates layer and an 18-cm dry substrate layer (SC18-NCA6 and SP18-RCA6) could be considered as the optimum system for the rooftop by simultaneously increasing the thickness of green roof layers, while applying low load to the top of structures, causing an advantage from the viewpoint of structural design [18].

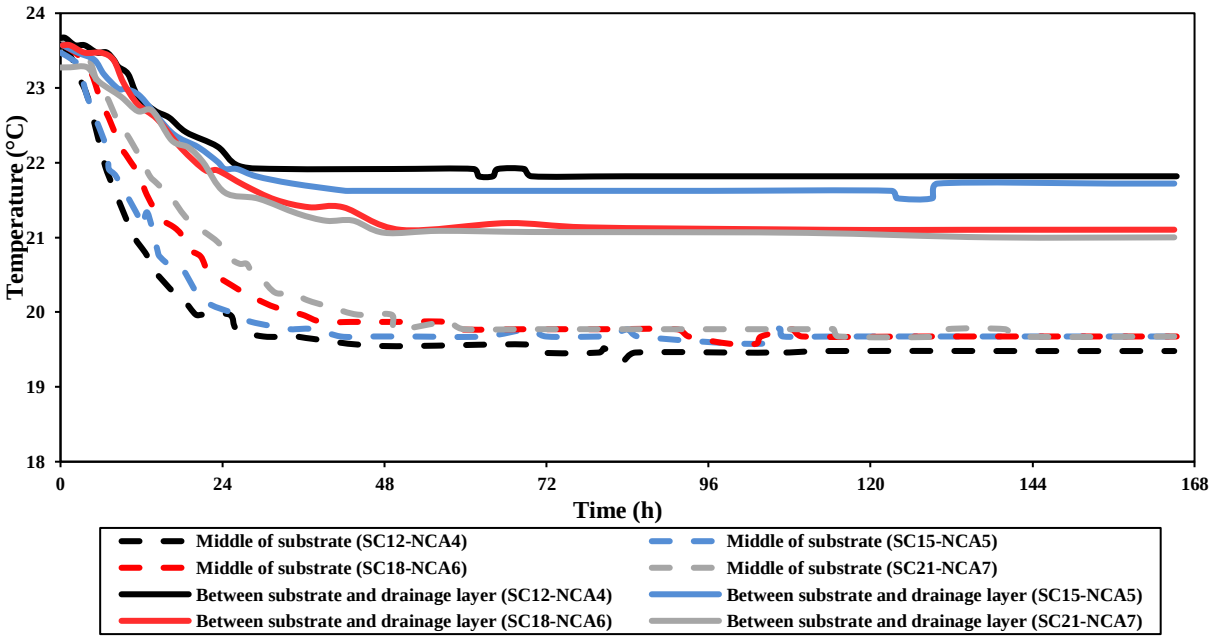

Fig. 17. Temperature distribution in the control models (change in the drainage and substrate layers' depth).

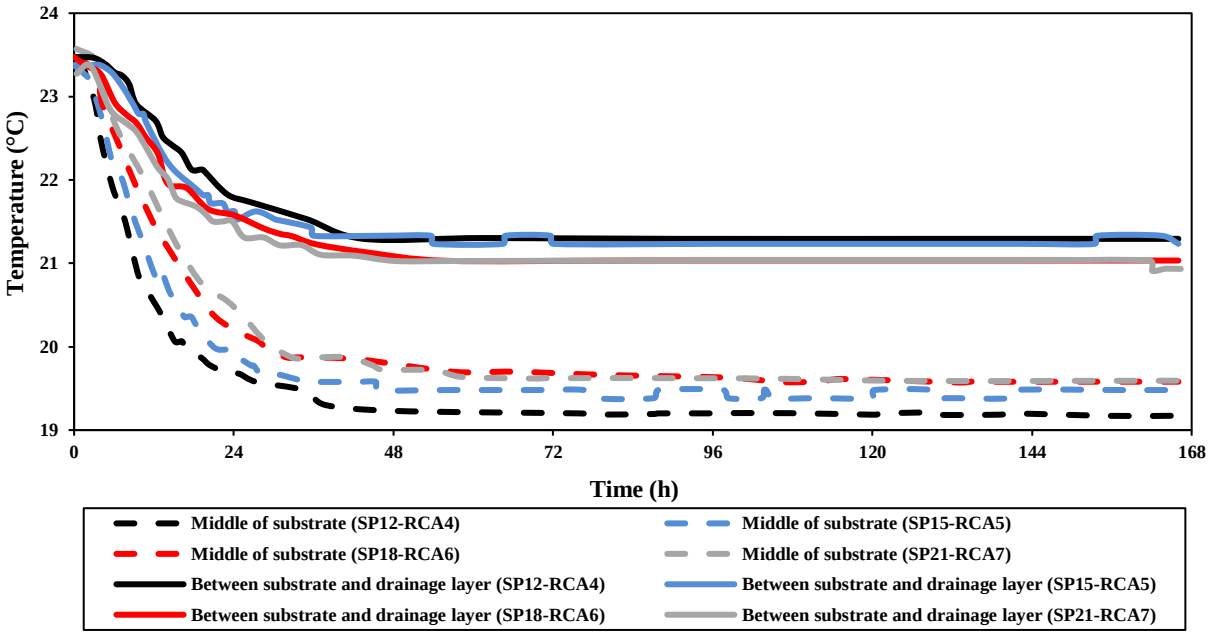

Fig. 18. Temperature distribution in the proposed models (change in the drainage and substrate layers' depth).

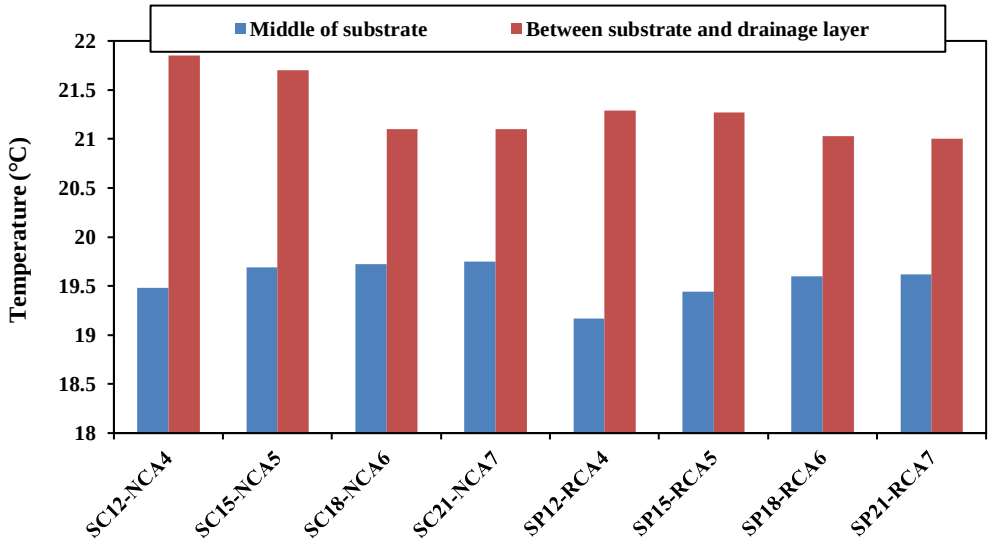

Fig. 19. Temperature in depth of green roof models (change in the drainage and substrate layers' depth).

5. Conclusions

This study dealt with the optimization of green roof made with the dry substrate layer and drainage layer of natural and recycled coarse aggregates, which were tested based on ISO 9869-1 [51] and simulated using the WUFI software. The optimized green roof's thermal behaviour was

also assessed through numerical simulations. The mini experimental green roof specimens and the developed 2D models produced the following conclusions:

- The thermal insulation performance of drainage layer was highly affected by the air-voids among coarse aggregates and no difference was pointed out between the Rc-value of natural coarse aggregate layer (NCA5) and recycled coarse aggregate layer (RCA5) owing to the heat resistance effect of air-voids, dominating the one of coarse aggregates types.
- The Rc-value of the SP15 was slightly lower than that of the SC15, demonstrating that the heat resistance ability of porous coarse recycled materials was slightly lower than that of dry soil particles. Therefore, it can be assumed that there is more air trapped within the former than within the latter, even though the difference between the Rc-value of SP15 and SC15 is not substantial.
- The narrow difference between the thermal resistance of the SC15 and SP15 caused the Rc-value of the proposed green roof specimen, SP15-RCA5, to be slightly lower than the one of the control green roof specimen, SC15-NCA5, (5.3%). In addition, considering the same thickness for the coarse aggregates layer and the dry substrate, the former has better thermal insulation performance than the latter, even though the Rc-value of the dry substrates (SC15 and SP15) is about twice greater than the one of the coarse aggregates layers (NCA5 and RCA5) due to a thicker layer of dry substrate than of coarse aggregates.
- The temperature distributions obtained though the simulations performed using the WUFI software presented similar trends (less than 2.6% difference) to the temperature distributions measured experimentally on the green roof specimens. This allowed for the model to be considered valid to simulate the studied configuration.
- The heat retention capacity of the green roof system increased when the thickness of the layers increased until a certain point. Any increase over 6 cm in the thickness of the drainage layer or any increase over 18 cm for the substrate layer didn't yield any increase in heat retention capacity as attested by the absence of changes in the temperature distribution. Therefore, SC15-NCA6 and SP15-RCA6 models were the best configuration while the dry substrate layer's depth was assumed constant (15 cm). In addition, when the thickness of coarse aggregates layer was assumed constant, the models with 18-cm dry substrate layer (SC18-NCA5 and SP18-RCA5)were the best configuration for the rooftops.
- By simultaneously increasing the thickness of green roof layers, the green roof with 18-cm dry substrate layer and 6-cm coarse aggregates layer was introduced as the best configuration either for the control model (SC18-NCA6) or for the proposed model (SP18-RCA6).
- In general, the difference between the Rc-value of the proposed and the control green roofs was not significant (5.3%). On the other hand, the weight of the proposed and the

control green roofs with optimized layers (SC18-NCA6 and SP18-RCA6) was the same (240 kg/m^2). Therefore, both control and proposed green roofs provided nearly the same thermal resistance for rooftops and applied the same dead load on the top of buildings. However, to reduce the burden on the environment and save natural resources, the use of green roof with recycled materials and optimized thicknesses of the different layers is recommended.

Acknowledgement

This research was funded through the University of Liège (ULiège) and the ARC grant for Concerted Research Actions, financed by the French Community of Belgium, Wallonia-Brussels Federation (CityRoof project: *Analogous green roofs for urban ecosystem services* (2020-2023)).

References

[1] J. Coma, G. Pérez, C. Solé, A. Castell, L.F. Cabeza, Thermal assessment of extensive green roofs as passive tool for energy savings in buildings, Renew. Energy. 85 (2016) 1106–1115.

[2] Directive, Directive 2010/31/eu of the European parliament and of the council of 19 May 2010 on the energy performance of buildings. Available from: http://www.epbd-ca.eu. Accessed 5 Mar 2013., (2010).

[3] G.A. Florides, S.A. Kalogirou, S.A. Tassou, L.C. Wrobel, Modeling of the modern houses of Cyprus and energy consumption analysis, Energy. 25 (2000) 915–937. https://doi.org/10.1016/S0360-5442(00)00030-X.

[4] R. Madandoust, M. Kazemi, P.K. Talebi, J. de Brito, Effect of the curing type on the mechanical properties of lightweight concrete with polypropylene and steel fibres, Constr. Build. Mater. 223 (2019) 1038–1052.

[5] M. Nematzadeh, J. Dashti, B. Ganjavi, Optimizing compressive behavior of concrete containing fine recycled refractory brick aggregate together with calcium aluminate cement and polyvinyl alcohol fibers exposed to acidic environment, Constr. Build. Mater. 164 (2018) 837–849. https://doi.org/10.1016/j.conbuildmat.2017.12.230.

[6] M. Santamouris, A. Argiriou, E. Dascalaki, C. Balaras, A. Gaglia, Energy characteristics and savings potential in office buildings, Sol. Energy. 52 (1994) 59–66. https://doi.org/10.1016/0038-092X(94)90081-C.

[7] A.A. Shahmansouri, H. Akbarzadeh Bengar, H. AzariJafari, Life cycle assessment of eco-friendly concrete mixtures incorporating natural zeolite in sulfate-aggressive environment, Constr. Build. Mater. 268 (2021) 121136. https://doi.org/10.1016/j.conbuildmat.2020.121136.

[8] G. Zhang, B.-J. He, B.J. Dewancker, The maintenance of prefabricated green roofs for preserving cooling performance: A field measurement in the subtropical city of Hangzhou, China, Sustain. Cities Soc. (2020) 102314.

[9] H. AzariJafari, J. Gregory, R. Kirchain, Potential Contribution of Deflection-Induced Fuel Consumption to US Greenhouse Gas Emissions, Transp. Res. Rec. 2674 (2020) 931–937.

[10] K. Fabbri, L. Tronchin, F. Barbieri, Coconut fibre insulators: The hygrothermal behaviour in the case of green roofs, Constr. Build. Mater. 266 (2021) 121026. https://doi.org/10.1016/j.conbuildmat.2020.121026.

[11] M. Kazemi, L. Courard, Modelling thermal and humidity transfers within green roof systems: effect of rubber crumbs and volcanic gravel, Adv. Build. Energy Res. 0 (2020) 1–26. https://doi.org/10.1080/17512549.2020.1858961.

[12] A. Tadeu, N. Simões, R. Almeida, C. Manuel, Drainage and water storage capacity of insulation cork board applied as a layer on green roofs, Constr. Build. Mater. 209 (2019) 52–65. https://doi.org/10.1016/j.conbuildmat.2019.03.073.
[13] A. Bellazzi, B. Barozzi, M.C. Pollastro, I. Meroni, Thermal resistance of growing media for green roofs: To what extent does the absence of specific reference values potentially affect the global thermal resistance of the green roof? An experimental example, J. Build. Eng. 28 (2020) 101076.
[14] X. Hao, Q. Xing, P. Long, Y. Lin, J. Hu, H. Tan, Influence of vertical greenery systems and green roofs on the indoor operative temperature of air-conditioned rooms, J. Build. Eng. 31 (2020) 101373. https://doi.org/10.1016/j.jobe.2020.101373.
[15] M. Kazemi, I. Boukhelkhal, P. Kosinski, S. Attia, Heat and moisture transfer measurement protocols for building envelopes, Sustainable Building Design Lab, 2021. https://doi.org/10.13140/RG.2.2.30642.53445.
[16] E. Oberndorfer, J. Lundholm, B. Bass, R.R. Coffman, H. Doshi, N. Dunnett, S. Gaffin, M. Köhler, K.K. Liu, B. Rowe, Green roofs as urban ecosystems: ecological structures, functions, and services, BioScience. 57 (2007) 823–833.
[17] B. Raji, M.J. Tenpierik, A. van den Dobbelsteen, The impact of greening systems on building energy performance: A literature review, Renew. Sustain. Energy Rev. 45 (2015) 610–623.
[18] A. Teemusk, Ü. Mander, Greenroof potential to reduce temperature fluctuations of a roof membrane: a case study from Estonia, Build. Environ. 44 (2009) 643–650.
[19] S. Cascone, F. Catania, A. Gagliano, G. Sciuto, A comprehensive study on green roof performance for retrofitting existing buildings, Build. Environ. 136 (2018) 227–239.
[20] P.C. Tabares-Velasco, M. Zhao, N. Peterson, J. Srebric, R. Berghage, Validation of predictive heat and mass transfer green roof model with extensive green roof field data, Ecol. Eng. 47 (2012) 165–173.
[21] M. Wanielista, M. Kelly, M. Hardin, A Comparative analysis of greenroof designs including depth of media, drainage layer materials, and pollution control media, Fla. Dep. Environ. Prot. Tallahass. FL USA. (2008).
[22] S. Parizotto, R. Lamberts, Investigation of green roof thermal performance in temperate climate: A case study of an experimental building in Florianópolis city, Southern Brazil, Energy Build. 43 (2011) 1712–1722.
[23] M. Uhl, L. Schiedt, Green roof storm water retention–monitoring results, in: 11th Int. Conf. Urban Drain. Edinb. UK, 2008.
[24] K. Vijayaraghavan, U.M. Joshi, R. Balasubramanian, A field study to evaluate runoff quality from green roofs, Water Res. 46 (2012) 1337–1345.
[25] H. Akbarzadeh Bengar, A.A. Shahmansouri, N. Akkas Zangebari Sabet, K. Kabirifar, V. W.Y. Tam, Impact of elevated temperatures on the structural performance of recycled rubber concrete: Experimental and mathematical modeling, Constr. Build. Mater. 255 (2020) 119374. https://doi.org/10.1016/j.conbuildmat.2020.119374.
[26] M. Nematzadeh, A.A. Shahmansouri, M. Fakoor, Post-fire compressive strength of recycled PET aggregate concrete reinforced with steel fibers: Optimization and prediction via RSM and GEP, Constr. Build. Mater. 252 (2020) 119057. https://doi.org/10.1016/j.conbuildmat.2020.119057.
[27] A. Vila, G. Pérez, C. Solé, A.I. Fernández, L.F. Cabeza, Use of recycled rubber from tires as drainage layer in green roofs, Build. Environ. 48 (2012) 101–106.
[28] P. Nuaklong, A. Wongsa, K. Boonserm, C. Ngohpok, P. Jongvivatsakul, V. Sata, P. Sukontasukkul, P. Chindaprasirt, Enhancement of mechanical properties of fly ash geopolymer containing fine recycled concrete aggregate with micro carbon fiber, J. Build. Eng. 41 (2021) 102403. https://doi.org/10.1016/j.jobe.2021.102403.

[29] D.-H. Vo, M.D. Yehualaw, C.-L. Hwang, M.-C. Liao, K.-D. Tran Thi, Y.-F. Chao, Mechanical and durability properties of recycled aggregate concrete produced from recycled and natural aggregate blended based on the Densified Mixture Design Algorithm method, J. Build. Eng. 35 (2021) 102067. https://doi.org/10.1016/j.jobe.2020.102067.
[30] S. Yousefi Moghadam, M.M. Ranjbar, R. Madandoust, M. Kazemi, Analytical study on the behavior of corrosion-damaged reinforced concrete beams strengthen with FRP, Rev. Romana Mater. 47 (2017) 514–521.
[31] S. Jahandari, Z. Tao, M. Saberian, M. Shariati, J. Li, M. Abolhasani, M. Kazemi, A. Rahmani, M. Rashidi, Geotechnical properties of lime-geogrid improved clayey subgrade under various moisture conditions, Road Mater. Pavement Des. 0 (2021) 1–19. https://doi.org/10.1080/14680629.2021.1950816.
[32] M. Tayebi, M. Nematzadeh, Post-fire flexural performance and microstructure of steel fiber-reinforced concrete with recycled nylon granules and zeolite substitution, Structures. 33 (2021) 2301–2316. https://doi.org/10.1016/j.istruc.2021.05.080.
[33] F. Bisceglie, E. Gigante, M. Bergonzoni, Utilization of waste Autoclaved Aerated Concrete as lighting material in the structure of a green roof, Constr. Build. Mater. 69 (2014) 351–361. https://doi.org/10.1016/j.conbuildmat.2014.07.083.
[34] M. Kazemi, R. Madandoust, J. de Brito, Compressive strength assessment of recycled aggregate concrete using Schmidt rebound hammer and core testing, Constr. Build. Mater. 224 (2019) 630–638.
[35] P. Mehrabi, M. Shariati, K. Kabirifar, M. Jarrah, H. Rasekh, N.T. Trung, A. Shariati, S. Jahandari, Effect of pumice powder and nano-clay on the strength and permeability of fiber-reinforced pervious concrete incorporating recycled concrete aggregate, Constr. Build. Mater. 287 (2021) 122652. https://doi.org/10.1016/j.conbuildmat.2021.122652.
[36] M. Saberian, J. Li, S.T.Anupiya.M. Perera, G. Ren, R. Roychand, H. Tokhi, An experimental study on the shear behaviour of recycled concrete aggregate incorporating recycled tyre waste, Constr. Build. Mater. 264 (2020) 120266. https://doi.org/10.1016/j.conbuildmat.2020.120266.
[37] M. Kazemi, M. Hajforoush, P.K. Talebi, M. Daneshfar, A. Shokrgozar, S. Jahandari, M. Saberian, J. Li, In-situ strength estimation of polypropylene fibre reinforced recycled aggregate concrete using Schmidt rebound hammer and point load test, J. Sustain. Cem.-Based Mater. (2020) 1–18.
[38] Z. Zhao, L. Courard, S. Groslambert, T. Jehin, A. Léonard, X. Jianzhuang, Use of recycled concrete aggregates from precast block for the production of new building blocks: An industrial scale study, Resour. Conserv. Recycl. 157 (2020) 104786.
[39] A. Pianella, R.E. Clarke, N.S.G. Williams, Z. Chen, L. Aye, Steady-state and transient thermal measurements of green roof substrates, Energy Build. 131 (2016) 123–131. https://doi.org/10.1016/j.enbuild.2016.09.024.
[40] J. Coma, G. Pérez, A. Castell, C. Solé, L.F. Cabeza, Green roofs as passive system for energy savings in buildings during the cooling period: use of rubber crumbs as drainage layer, Energy Effic. 7 (2014) 841–849.
[41] M. Kazemi, L. Courard, Simulation of humidity and temperature distribution in green roof with pozzolana as drainage layer: influence of outdoor seasonal weather conditions and internal ceiling temperature, Sci. Technol. Built Environ. 27 (2021) 509–523.
[42] B. Schafaczek, D. Zirkelbach, Ermittlung von Materialeigenschaften und effektiven Übergangsparametern von Dachbegrünungen zur zuverlässigen Simulation der hygrothermischen Verhältnisse in und unter Gründächern bei beliebigen Nutzungen und unterschiedlichen Standorten:[Abschlussbericht], Fraunhofer-IRB-Verlag, 2013.
[43] M. Vertal', M. Zozulák, A. Vašková, A. Korjenic, Hygrothermal initial condition for simulation process of green building construction, Energy Build. 167 (2018) 166–176.

[44] D. Zirkelbach, S.-R. Mehra, K.-P. Sedlbauer, H.-M. Künzel, B. Stöckl, A hygrothermal green roof model to simulate moisture and energy performance of building components, Energy Build. 145 (2017) 79–91.
[45] M. Kazemi, L. Courard, S. Attia, Hygrothermal modeling of green roof made with substrate and drainage layers of coarse recycled materials, in: Bruges, Belgium, 2021: pp. 1–8.
[46] M. Kazemi, L. Courard, J. Hubert, Heat transfer measurement within green roof with incinerated municipal solid waste aggregates, Sustainability. 13 (2021) 7115. https://doi.org/10.3390/su13137115.
[47] O. Saadatian, K. Sopian, E. Salleh, C.H. Lim, S. Riffat, E. Saadatian, A. Toudeshki, M.Y. Sulaiman, A review of energy aspects of green roofs, Renew. Sustain. Energy Rev. 23 (2013) 155–168.
[48] M. Nematzadeh, A. Baradaran-Nasiri, M. Hosseini, Effect of pozzolans on mechanical behavior of recycled refractory brick concrete in fire, Struct. Eng. Mech. 72 (2019) 339–354. https://doi.org/10.12989/sem.2019.72.3.339.
[49] M. Kazemi, M. Hajforoush, P.K. Talebi, M. Daneshfar, A. Shokrgozar, S. Jahandari, M. Saberian, J. Li, In-situ strength estimation of polypropylene fibre reinforced recycled aggregate concrete using Schmidt rebound hammer and point load test, J. Sustain. Cem.-Based Mater. 9 (2020) 289–306. https://doi.org/10.1080/21650373.2020.1734983.
[50] M. Kazemi, L. Courard, Modelling hygrothermal conditions of unsaturated substrate and drainage layers for the thermal resistance assessment of green roof: Effect of coarse recycled materials, Energy Build. 250 (2021) 111315. https://doi.org/10.1016/j.enbuild.2021.111315.
[51] ISO 9869-1, Thermal insulation, Building elements, In-situ measurement of thermal resistance and thermal transmittance-Part 1: Heat flow meter method, Lond. BSI. (2014).
[52] S. Cascone, Green Roof Design: State of the Art on Technology and Materials, Sustainability. 11 (2019) 3020. https://doi.org/10.3390/su11113020.
[53] H. Ling, C. Chen, H. Qin, S. Wei, J. Lin, N. Li, M. Zhang, N. Yu, Y. Li, Indicators evaluating thermal inertia performance of envelops with phase change material, Energy Build. 122 (2016) 175–184. https://doi.org/10.1016/j.enbuild.2016.04.009.
[54] N. Simões, R. Almeida, A. Tadeu, M. Brett, J. Almeida, Comparison between cork-based and conventional green roof solutions, Build. Environ. 175 (2020) 106812. https://doi.org/10.1016/j.buildenv.2020.106812.
[55] B. Dvorak, A. Volder, Rooftop temperature reduction from unirrigated modular green roofs in south-central Texas, Urban For. Urban Green. 12 (2013) 28–35.
[56] G. Vesuviano, V. Stovin, A generic hydrological model for a green roof drainage layer, Water Sci. Technol. 68 (2013) 769–775.
[57] EN 12620, Aggregates for concrete. European Committee for Standardization, ITeh Stand. Store. (2013). https://standards.iteh.ai/catalog/standards/cen/aef412e6-36ce-49d3-afaa-5200d721ff84/en-12620-2013 (accessed January 19, 2021).
[58] I.A. Atsonios, I.D. Mandilaras, D.A. Kontogeorgos, M.A. Founti, A comparative assessment of the standardized methods for the in–situ measurement of the thermal resistance of building walls, Energy Build. 154 (2017) 198–206.
[59] G. Desogus, S. Mura, R. Ricciu, Comparing different approaches to in situ measurement of building components thermal resistance, Energy Build. 43 (2011) 2613–2620.
[60] A. Rodler, S. Guernouti, M. Musy, Bayesian inference method for in situ thermal conductivity and heat capacity identification: Comparison to ISO standard, Constr. Build. Mater. 196 (2019) 574–593.
[61] M. Krus, Moisture transport and storage coefficients of porous mineral building materials: Theoretical principles and new test methods, Fraunhofer IRB Verlag Stuttgart, 1996.

[62] EN 1015-19, Methods of test for mortar for masonry. Determination of water vapour permeability of hardened rendering and plastering mortars, (1999).
[63] Engineering ToolBox, Specific Heat of some common Substances, (2003). https://www.engineeringtoolbox.com/specific-heat-capacity-d_391.html (accessed January 19, 2021).
[64] IES VE, Thermal Conductivity, Specific Heat Capacity and Density, (2018). https://help.iesve.com/ve2018/table_6_thermal_conductivity__specific_heat_capacity_and_density.htm (accessed January 19, 2021).
[65] ASTM D4611 - 16, Standard test method for specific heat of rock and soil, ASTM International, 2018. https://doi.org/10.1520/D4611-16.
[66] P.P. Urone, R. Hinrichs, College Physics: OpenStax, (2018).
[67] S.A. Taylor, R.D. Jackson, Heat capacity and specific heat, Methods Soil Anal. Part 1 Phys. Mineral. Methods. 5 (1986) 941–944.
[68] K.A. Alnefaie, N.H. Abu-Hamdeh, Specific heat and volumetric heat capacity of some saudian soils as affected by moisture and density, in: Int. Conf. Mech. Fluids Heat Elast. Electromagn. Fields, 2013: pp. 139–143.
[69] D.J. Sailor, M. Hagos, An updated and expanded set of thermal property data for green roof growing media, Energy Build. 43 (2011) 2298–2303. https://doi.org/10.1016/j.enbuild.2011.05.014.
[70] F. Hu, S. Wu, Y. Sun, Hollow-Structured Materials for Thermal Insulation, Adv. Mater. 31 (2019) 1801001.
[71] B.M. Suleiman, J. Larfeldt, B. Leckner, M. Gustavsson, Thermal conductivity and diffusivity of wood, Wood Sci. Technol. 33 (1999) 465–473.
[72] X. Zhou, F. Zheng, H. Li, C. Lu, An environment-friendly thermal insulation material from cotton stalk fibers, Energy Build. 42 (2010) 1070–1074. https://doi.org/10.1016/j.enbuild.2010.01.020.
[73] J. Coma, G. Pérez, A. Castell, C. Solé, L.F. Cabeza, Green roofs as passive system for energy savings in buildings during the cooling period: use of rubber crumbs as drainage layer, Energy Effic. 7 (2014) 841–849.
[74] M. Eksi, D.B. Rowe, I.S. Wichman, J.A. Andresen, Effect of substrate depth, vegetation type, and season on green roof thermal properties, Energy Build. 145 (2017) 174–187. https://doi.org/10.1016/j.enbuild.2017.04.017.